



Bragg resonance in microfiber realized by two-photon polymerization

JIA WANG,^{1,4} CHUPAO LIN,^{1,4} CHANGRUI LIAO,^{1,*} ZONGSONG GAN,²
ZHENGYONG LI,¹ SHEN LIU,¹ LEI XU,³ YING WANG,¹ JUN HE,¹ YIPING
WANG,¹

¹Key Laboratory of Optoelectronic Devices and Systems of Ministry of Education and Guangdong Province, College of Optoelectronic Engineering, Shenzhen University, Shenzhen 518060, China

²Wuhan National Laboratory for Optoelectronics (WNLO), Huazhong University of Science and Technology (HUST), Wuhan 430074, China

³School of Electronic and Communication Engineering, Shenzhen Polytechnic, Shenzhen 518055, China

⁴These authors contributed equally to this work

*cliao@szu.edu.cn

Abstract: A new method for microfiber Bragg gratings (μ -FBGs) fabrication by means of two-photon polymerization in photosensitive resin is reported. Such polymerized μ -FBGs were cured along with the surface of microfibers without any damage or distortion to the substrate. The laser intensity was optimized to improve the spectral properties of the polymerized gratings. The refractive index measurement was performed and the maximum sensitivity obtained is ~ 207 nm/RIU at the refractive index value of 1.440 with the fiber diameter being 1.7 μ m. This work opens a new idea for optical structure integration and further optical functionality integration.

© 2018 Optical Society of America under the terms of the [OSA Open Access Publishing Agreement](#)

OCIS codes: (060.3735) Fiber Bragg gratings; (060.2370) Fiber optics sensors; (230.4000) Microstructure fabrication.

References and links

1. X. Guo and L. Tong, "Supported microfiber loops for optical sensing," *Opt. Express* **16**(19), 14429–14434 (2008).
2. G. Brambilla, V. Finazzi, and D. Richardson, "Ultra-low-loss optical fiber nanotapers," *Opt. Express* **12**(10), 2258–2263 (2004).
3. L. Tong, R. R. Gattass, J. B. Ashcom, S. He, J. Lou, M. Shen, I. Maxwell, and E. Mazur, "Subwavelength-diameter silica wires for low-loss optical wave guiding," *Nature* **426**(6968), 816–819 (2003).
4. J. L. Kou, M. Ding, J. Feng, Y. Q. Lu, F. Xu, and G. Brambilla, "Microfiber-based Bragg gratings for sensing applications: a review," *Sensors (Basel)* **12**(7), 8861–8876 (2012).
5. A. Iadicco, A. Cusano, A. Cutolo, R. Bernini, and M. Giordano, "Thinned fiber Bragg gratings as high sensitivity refractive index sensor," *IEEE Photonics Technol. Lett.* **16**(4), 1149–1151 (2004).
6. X. Fang, C. R. Liao, and D. N. Wang, "Femtosecond laser fabricated fiber Bragg grating in microfiber for refractive index sensing," *Opt. Lett.* **35**(7), 1007–1009 (2010).
7. C. Liao, D. N. Wang, Y. Li, T. Sun, and K. T. V. Grattan, "Temporal thermal response of Type II-IR fiber Bragg gratings," *Appl. Opt.* **48**(16), 3001–3007 (2009).
8. C. R. Liao, Y. H. Li, D. N. Wang, T. Sun, and K. T. V. Grattan, "Morphology and Thermal Stability of Fiber Bragg Gratings for Sensor Applications Written in H₂-Free and H₂-Loaded Fibers by Femtosecond Laser," *IEEE Sens. J.* **10**(11), 1675–1681 (2010).
9. Y. Ran, Y. N. Tan, L. P. Sun, S. Gao, J. Li, L. Jin, and B. O. Guan, "193 nm excimer laser inscribed Bragg gratings in microfibers for refractive index sensing," *Opt. Express* **19**(19), 18577–18583 (2011).
10. M. Ding, M. N. Zervas, and G. Brambilla, "A compact broadband microfiber Bragg grating," *Opt. Express* **19**(16), 15621–15626 (2011).
11. K. P. Nayak, F. Le Kien, Y. Kawai, K. Hakuta, K. Nakajima, H. T. Miyazaki, and Y. Sugimoto, "Cavity formation on an optical nanofiber using focused ion beam milling technique," *Opt. Express* **19**(15), 14040–14050 (2011).
12. B. H. Cumpston, S. P. Ananthavel, S. Barlow, D. L. Dyer, J. E. Ehrlich, L. L. Erskine, A. A. Heikal, S. M. Kuebler, I. Y. S. Lee, D. M. Maughon, J. Qin, H. Röckel, M. Rumi, X. L. Wu, S. R. Marder, and J. W. Perry, "Two-photon polymerization initiators for three-dimensional optical data storage and microfabrication," *Nature* **398**(6722), 51–54 (1999).

13. S. Kawata, H. B. Sun, T. Tanaka, and K. Takada, "Finer features for functional microdevices," *Nature* **412**(6848), 697–698 (2001).
14. S. Maruo, A. Takaura, and Y. Saito, "Optically driven micropump with a twin spiral microrotor," *Opt. Express* **17**(21), 18525–18532 (2009).
15. A. Ovsianikov, B. Chichkov, P. Mente, N. A. Monteiro-Riviere, A. Doraiswamy, and R. J. Narayan, "Two Photon Polymerization of Polymer&Ceramic Hybrid Materials for Transdermal Drug Delivery," *Appl. Ceram. Tech.* **4**(1), 22–29 (2007).
16. S. Maruo, K. Ikuta, and H. Korogi, "Submicron manipulation tools driven by light in a liquid," *Appl. Phys. Lett.* **82**(1), 133–135 (2003).
17. L. P. C. Gomez, A. Spangenberg, X. A. Ton, Y. Fuchs, F. Bokeloh, J. P. Malval, B. Tse Sum Bui, D. Thuau, C. Ayela, K. Haupt, and O. Soppera, "Rapid Prototyping of Chemical Microsensors Based on Molecularly Imprinted Polymers Synthesized by Two-Photon Stereolithography," *Adv. Mater.* **28**(28), 5931–5937 (2016).
18. G. Brambilla, F. Xu, P. Horak, Y. Jung, F. Koizumi, N. P. Sessions, E. Koukharenko, X. Feng, G. S. Murugan, J. S. Wilkinson, and D. J. Richardson, "Optical fiber nanowires and microwires: fabrication and applications," *Adv. Opt. Photonics* **1**(1), 107–161 (2009).
19. Y. L. Zhang, Q. D. Chen, H. Xia, and H. B. Sun, "Designable 3D nanofabrication by femtosecond laser direct writing," *Nano Today* **5**(5), 435–448 (2010).
20. I. P. Arjona, G. J. de Valcarcel, and E. Roldan, "Two-photon absorption," *Rev. Mex. Fis.* **49**(1), 92–101 (2003).
21. K. S. Lee, R. H. Kim, D. Y. Yang, and S. H. Park, "Advances in 3D nano/microfabrication using two-photon initiated polymerization," *Prog. Polym. Sci.* **33**(6), 631–681 (2008).
22. C. Liao, Q. Wang, L. Xu, S. Liu, J. He, J. Zhao, Z. Li, and Y. Wang, "D-shaped fiber grating refractive index sensor induced by an ultrashort pulse laser," *Appl. Opt.* **55**(7), 1525–1529 (2016).
23. C. Lin, C. Liao, J. Wang, J. He, Y. Wang, Z. Li, T. Yang, F. Zhu, K. Yang, Z. Zhang, and Y. Wang, "Fiber surface Bragg grating waveguide for refractive index measurements," *Opt. Lett.* **42**(9), 1684–1687 (2017).

1. Introduction

Microfiber is an important substrate for photonic devices in optical fiber communication and optical fiber sensing due to its intrinsic properties, i.e. large evanescent field, small mode-field area, high nonlinearity and low-loss connection with single-mode fiber (SMF) [1–4]. The advent of microfiber provides a new platform for fiber Bragg gratings (FBGs) with extended functions. Nowadays, a variety of microfiber Bragg gratings (μ -FBGs) based on structural change or refractive index modulation of material have been successfully fabricated by use of different fabrication methods, i.e. chemical etching [5], femtosecond (Fs) laser micromachining [6–8], ultraviolet (UV) laser irradiation [9], and focused ion beam milling [10,11]. However, in the mentioned works, the Bragg resonances are realized by introducing structural damage to microfibers or RI modulation in the microfibers.

Currently, two-photon polymerization (TPP) induced by near-infrared Fs laser has become a powerful fabrication method for the preparation of 3-D fine structure with a feature size beyond optical diffraction limit [12]. Since the micro-bull was realized by TPP [13], different kinds of applications of TPP have sprung up, i.e. microfluidic devices [14], biomedical structures [15], MEMS [13, 16, 17].

In this work, we report a new method for μ -FBG fabrication by use of TPP in photosensitive resin. The designed grating is polymerized along with the surface of microfiber and the formed grating exhibits great bonding strength with the microfiber. The Bragg resonance is excited in the microfiber by the polymerized grating and successfully used for liquid RI measurement. The maximum RI sensitivity obtained is ~ 207 nm/RIU at the RI of 1.440 with the fiber diameter being $1.7 \mu\text{m}$. This work not only demonstrates a new method of fiber grating fabrication, but also a new idea for optical structure integration and further optical functionality integration. It has laid a foundation work for subsequent research on functional structure polymerized on or in the fiber.

2. Experimental setup

The experimental setup of μ -FBG fabrication is demonstrated in Fig. 1(a). Fs laser beam (800 nm, 120 fs, 80 MHz) is firstly expanded and then focused in the interface between the microfiber and the photosensitive resin by use of an oil-immersion microscope objective (MO) with a NA value of 1.25. The laser focus size is $\sim 0.78 \mu\text{m}$. The laser intensity is precisely adjusted by a variable attenuator comprised by a $\lambda/2$ wave plate (W) and a Glan-

prism polarizer (P). The laser irradiation time is controlled by use of a PC-driven mechanical shutter. As shown in Fig. 1(b), the machined microfiber immersed in the photosensitive resin, which is sandwiched between cover and slide glasses, is mounted on 3-D translation stage (Newport, XMS50/XMS50/GTS30V). Normally, the fiber diameter used in the experiment is less than $4\mu\text{m}$. To achieve a uniform photosensitive resin on the microfiber, one layer of tape with a thickness of $50\mu\text{m}$ is stuck to the edge of the slide glass to support the microfiber to ensure sufficient space for grating inscription. The CCD mounted above is used to monitor the fabrication process. The schematic diagram of the polymerized μ -FBG is illustrated in Fig. 1(c), where the green and blue parts denote the polymerized grating structure and the microfiber, respectively.

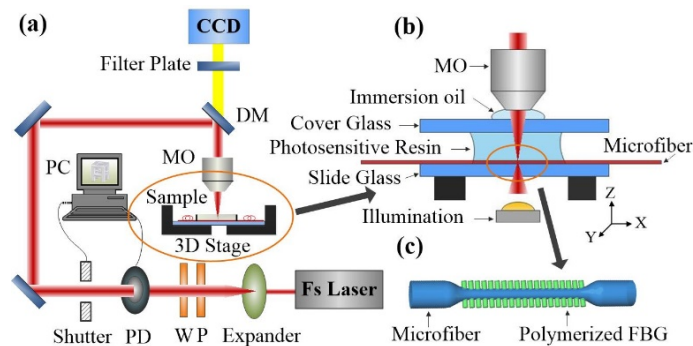


Fig. 1. (a) Experimental setup of two-photon polymerization for fiber grating fabrication. (b) Microfiber fixing method during two-photon polymerization fabrication. (c) Schematic diagram of the polymerized μ -FBG.

3. Results and discussion

In this work the microfiber is fabricated by use of flame-tapering method [18], where hydro-oxygen flame is used to soften the SMF and two motorized translation stages are used to simultaneously stretch the fiber. By precisely controlling the relative moving direction and speed of two translation stages, we can obtain the microfiber with the designed length and diameter. In order to ensure enough mechanical strength of the μ -FBG, the microfiber with a diameter of $\sim 2\mu\text{m}$ is drawn for the grating fabrication.

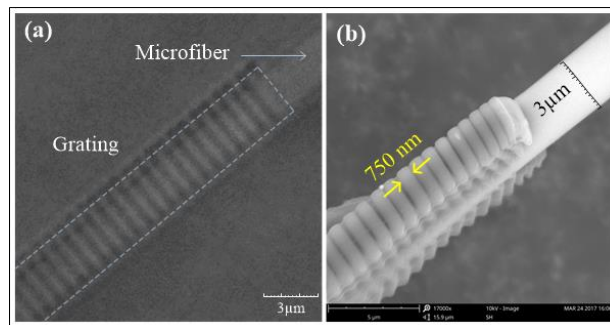


Fig. 2. (a) Optical microscope image of the polymerized grating before rinsing. (b) SEM image of the structure after rinsing.

The photosensitive resin used is a negative photoresist (type: PP-1, purchased from Zhichu optics Co., Ltd., Shenzhen, China), which contains photo-initiator (IGR-369, Ciba-Geigy) and monomer (SR444, SR368, from Sartomer) for polymerization [19]. TPP excited by Fs laser can introduce cross-linking of polymer chains through radical polymerization, making the exposed region insoluble to the solvent, therefore the structure can be printed and formed on the substrate. During the polymerization, the fluorescence can be observed in the

focal point of laser beam due to the nonlinear light-matter interaction [20]. The refractive index of the photosensitive resin before and after curing are ~ 1.51 and ~ 1.53 around 1500 nm. Since the RI of photosensitive resin is slightly changed due to polymerization, the polymerized grating structure can be easily observed during laser fabrication.

The grating is printed by use of line-by-line inscription, where the laser focal point is fixed and the microfiber is firstly translated along the radial direction of the fiber with the designed velocity and distance. After inscription of the first grating segment, the laser beam is blocked and the microfiber is then translated to the starting point of the next grating segment, after which the cycle is repeated. When the laser fabrication is completed, the cover slide above the microfiber is carefully taken away and the polymerized structure is successively rinsed by use of isopropanol for 10 s and then alcohol for 30 s. Figure 2(a) shows the optical microscope image of the polymerized fiber grating before rinsing and Fig. 2(b) shows the scanning electron microscopy (SEM) image of this structure after rinsing. It can be seen from Fig. 2(b) that the polymerized grating segments appear as plate array, which are tightly attached to the two sides of the microfiber.

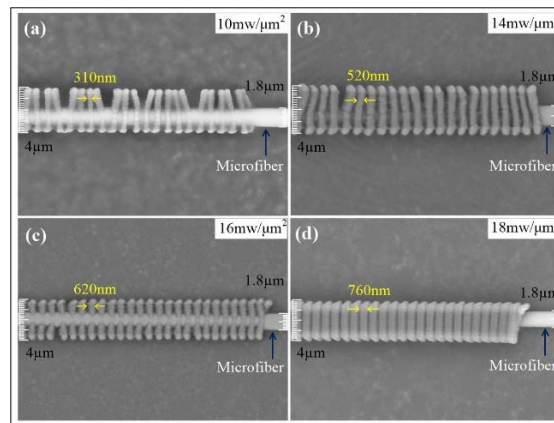


Fig. 3. SEM images of the polymerized μ -FBGs with Fs laser intensities of $10 \text{ mw}/\mu\text{m}^2$ (a), $14 \text{ mw}/\mu\text{m}^2$ (b), $16 \text{ mw}/\mu\text{m}^2$ (c) and $18 \text{ mw}/\mu\text{m}^2$ (d).

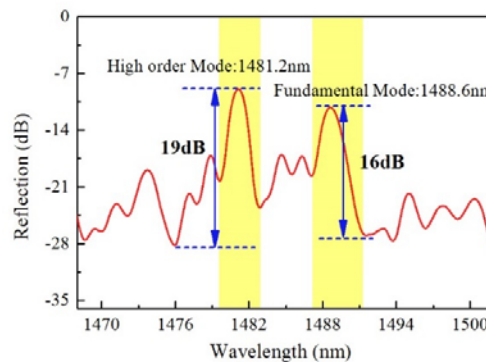


Fig. 4. Reflection spectrum of the polymerized μ -FBG in Fig. 3(d).

The laser intensity plays an important role in grating fabrication. There is a certain threshold of laser intensity for solidification of the photosensitive resin after polymerization and the absorption rate of laser intensity for the resin is proportional to square of the laser intensity [21]. Low laser intensity will produce small polymer voxel and therefore the bonding force between the polymerized grating and the microfiber is weak, resulting in structural deformation of the polymerized grating. Conversely, excessively high laser

intensity will introduce large polymer voxel and the adjacent grating segments overlap and therefore the microfiber might be totally wrapped in the cured resin. This can increase the duty cycle of grating and weaken its RI modulation. Experiments have been made to optimize the laser intensity for grating fabrication. The microfiber with a diameter of $\sim 1.8 \mu\text{m}$ is translated at a speed of $8 \mu\text{m/s}$ to create the grating with a pitch of $1.07 \mu\text{m}$, and the laser intensity is increased from $10 \text{ mw}/\mu\text{m}^2$ to $18 \text{ mw}/\mu\text{m}^2$. The expose time of each grating segment was 0.5s .

Figure 3 shows SEM images of the polymerized gratings fabricated by different laser intensity from the top view (along the laser irradiation direction). It can be seen from this figure that when the laser intensity rises from $10 \text{ mw}/\mu\text{m}^2$ to $18 \text{ mw}/\mu\text{m}^2$ the line width of grating segment is increased from 310 nm to 760 nm . When the laser intensity is lower than $16 \text{ mw}/\mu\text{m}^2$, the polymerized gratings exhibit different degrees of structural deformation as shown in Figs. 3(a)-3(c). When the laser intensity is increased up to $18 \text{ mw}/\mu\text{m}^2$, as shown in figure. 3(d), the grating segments turn into a robust and uniform rod array being perpendicular to the microfiber. Among the four μ -FBGs in Fig. 3, typical Bragg resonance can be observed only for the last one.

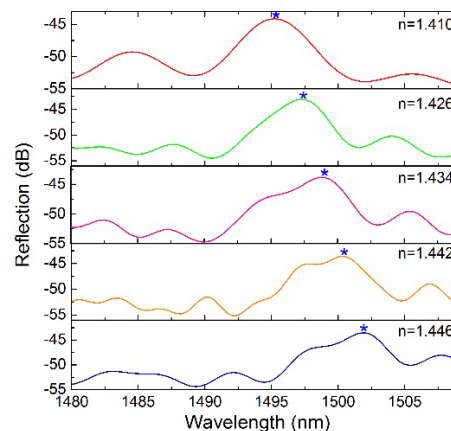


Fig. 5. Reflection spectral evolution of the polymerized μ -FBG in environmental RI measurement.

The reflection spectrum of the polymerized μ -FBG in Fig. 3(d) has been measured by use of a broadband light source and an optical spectrum analyzer with a resolution of 0.5 nm . The reflection spectrum of the μ -FBG in air is demonstrated in Fig. 4, where there are two main Bragg resonant peaks at 1488.6 nm ($\sim 16 \text{ dB}$) and 1481.2 nm ($\sim 19 \text{ dB}$), which are corresponding to the backward fundamental and high-order modes being coupled from the forward fundamental mode in the microfiber. The Bragg resonant peak is sensitive to surrounding RI change due to the enhanced evanescent field outside the microfiber.

The environmental RI response of the polymerized μ -FBG has been investigated at the room temperature ($22 \text{ }^\circ\text{C}$). The μ -FBG (grating pitch = $1.07 \mu\text{m}$; pitch number = 500) is polymerized along the microfiber with a diameter of $4 \mu\text{m}$. During the measurement the μ -FBG was sequentially immersed into a series of RI oil (Cargille Lab) with RI value from 1.380 to 1.446 by an interval of 0.004. The μ -FBG needs to be fully cleaned with alcohol after each measurement and a new round of measurement can be performed only when the spectrum restores to the original state in air. Figure 5 shows reflection spectral evolution of the polymerized μ -FBG immersed in different RI oils (1.410, 1.426, 1.434, 1.442, and 1.416). It can be seen from this figure that as the oil RI increases the Bragg resonant peak marked by asterisk exhibits a significant red shift and a slow degradation of resonant strength.

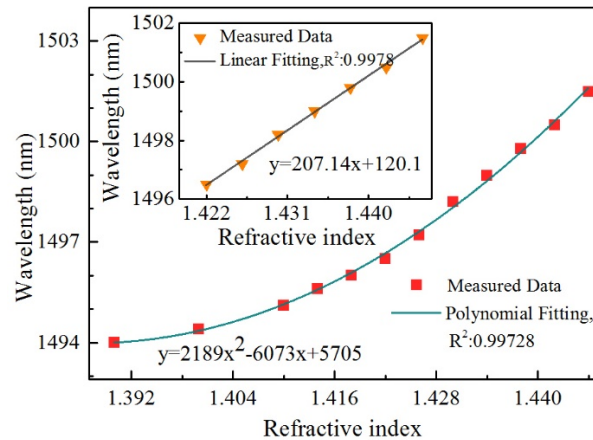


Fig. 6. Polynomial fitting relationship between Bragg wavelength and oil RI. Insert: partial linear relationship between Bragg wavelength and oil RI from 1.420 to 1.450.

Figure 6 shows the polynomial fitting relationship between the Bragg wavelength and the oil RI measured in Fig. 5. There is a small deviation between the measured data and the fitting curve that may be caused by measurement error of Bragg wavelength. It is noted that the evanescent field is enhanced when the RI value of oil is approaching to that of the silica microfiber. The inset of Fig. 6 shows a partial linear relationship between the Bragg wavelength and the oil RI from 1.420 to 1.450 and a RI sensitivity of ~ 207.14 nm/RIU is achieved at 1.446. The RI sensitivity of the polymerized μ -FBG reaches the superior level comparing with previously reported μ -FBGs of ~ 231.4 nm/RIU [6], ~ 30 nm/RIU [22] and ~ 16 nm/RIU [23], respectively.

4. Conclusion

In conclusion, TPP method is firstly used to fabricate grating structure along with the microfiber to excite the Bragg resonance in it. Fs laser intensity was firstly optimized to find out the best polymerization parameters and then the designed Bragg grating structures were polymerized along the microfiber. More than one Bragg resonant peak was observed in the reflection spectrum. Successively, we studied the environmental RI response of the polymerized μ -FBG and observed a nonlinear relationship between the Bragg wavelength and the oil RI, where the maximum sensitivity of ~ 207 nm/RIU is achieved at 1.446. Generally speaking, TPP method provides many possibilities for fabricating arbitrary 3-D structures and tailing their physical properties and many other functional structures besides μ -FBG can be polymerized on or in optical fiber for potential sensing applications.

Funding

National Natural Science Foundation of China (61575128, 61425007, 61635007, 61505120); Guangdong Natural Science Foundation (2015A030313541, 2015B010105007, 2014A030308007); Education Department of Guangdong Province (2015KTSCX119), Science and Technology Innovation Commission of Shenzhen (JCYJ20160520163134575, JCYJ20160523113602609, JCYJ20160427104925452); Development and Reform Commission of Shenzhen Municipality Foundation.